JOURNAL OF CATALYSIS 130, 597–610 (1991)

An Isotopic Tracer Study of the Deactivation of Ru/TiO_2 Catalysts during Fischer–Tropsch Synthesis

KAMALA R. KRISHNA AND ALEXIS T. BELL

Center for Advanced Materials, Lawrence Berkeley Laboratory, and Department of Chemical Engineering, University of California, Berkeley, California 94720

Received August 13, 1990; revised March 18, 1991

An investigation of the causes of catalyst deactivation during Fischer–Tropsch synthesis over Ru/TiO_2 catalysts has been carried out. The effects of Ru dispersion, TiO_2 phase, and TiO_2 surface area on catalyst activity and selectivity were examined. CO chemisorption capacity and carbon species accumulation were determined as a function of reaction time using isotopic tracer techniques in conjunction with temperature-programmed surface reaction (TPSR). The results of this investigation show that all of the catalysts undergo deactivation with time, with no change in product selectivity. Initially, deactivation is very rapid followed by a slower activity loss. The long-term rate of deactivation is proportional to the initial CO turnover frequency, obtained by extrapolation of the long-term activity data. Deactivation is accompanied by a progressive loss in CO chemisorption capacity as well as an accumulation of various types of carbon species. Carbidic carbon, C_α, and alkyl carbon chains, C_β, were observed to accumulate as reaction proceeds. C_β consists of two species, C'_β which is the precursor to C_{2+} hydrocarbon products and C''_β which consists of longer alkyl chains and does not participate in the production of gas phase products. The rapid initial loss in activity in the first 10 min correlates with the $C_\alpha + C_\beta$ accumulation; the long-term loss in CO uptake and catalyst activity are probably due to C''_β. The alkyl chains comprising C''_β do not undergo hydrogenolysis under reaction conditions, probably due to inaccessibility to hydrogen.

INTRODUCTION

A number of previous investigations have shown that while Ru exhibits a high specific activity for Fischer–Tropsch synthesis, it undergoes a progressive loss in activity that is accompanied by a build-up of carbonaceous species (*1–6*). Dalla Betta and co-workers (*1*, *2*) have ascribed the loss in activity of Ru/Al_2O_3 catalysts to the carbonaceous deposits, and have noted that the original activity of these catalysts could be restored by reduction in H_2. Similar observations have been reported by Everson *et al.* (*3*) and Ekerdt and Bell (*4*). These authors noted that the rate of deactivation was a function of reaction conditions. Using infrared spectroscopy, Ekerdt and Bell (*4*) and Yamasaki and co-workers (*7*) observed the accumulation of hydrocarbon species on the surface under reaction conditions. Ekerdt and Bell (*4*) concluded that the observed species did not function as reaction intermediates, since these species could only be removed by H_2 reduction in the absence of CO. Reduction of the catalyst following reaction demonstrated that during reaction, the catalyst had accumulated 1–6 Ru ML equivalents of carbon. Based on studies on a Ru/Al_2O_3 catalyst, Bowman and Bartholomew (*6*) have proposed a model for the rate of deactivation. According to this model, the rate of deactivation is proportional to the partial pressure of CO and the concentration of active sites. Temperature-programmed reaction of the catalyst after reaction produced a spectrum exhibiting two peaks. The first of these peaks occurred at 460 K and corresponded to the removal of 5 ML equivalents of car-

0021-9517/91 $3.00

bon, whereas the second peak occurred at 685 K and corresponded to the removal of 2.5 ML equivalents of carbon.

Isotopic tracer studies conducted in this laboratory (*8–14*) have demonstrated that two types of carbon are deposited on the surface of Ru particles supported on SiO_2 and TiO_2. The first is carbidic, or C_α, carbon. This species is produced by the dissociation of adsorbed CO and serves as a precursor to methane and C_{2+} hydrocarbons. The second form of carbon consists of short (3–5 carbon atoms) alkyl chains and is designated as C_β. By combining isotopic tracer techniques with temperature-programmed reaction, it has been shown that the C_β pool of carbon can be divided into two pools. The first of these pools is designated as C'_β, and corresponds to alkyl groups serving as intermediates to the C_{2+} hydrocarbons. The second pool of carbon, designated as C''_β, corresponds to longer alkyl chains which are not involved in the formation of reaction products. Under reaction conditions, the coverages of C_α and C'_β come to a steady state with time, whereas the accumulation of C''_β increases monotonically. Zhou and Gulari (*15*) have also found evidence for the presence of C_α and C_β during CO hydrogenation over Al_2O_3-supported Ru. The inventory of C_α was observed to go through a maximum with reaction time, whereas the inventory of C_β increased monotonically. In a subsequent study (*16*), the authors speculated that the low activity alkyl species that could be observed by infrared spectroscopy were located on sites surrounded by adsorbed CO.

The objective of this study was to characterize the deactivation of Ru/TiO_2 catalysts during Fischer–Tropsch synthesis and to identify the causes for the loss in activity. The influence of Ru dispersion, TiO_2 phase, and TiO_2 surface area were considered. The CO chemisorption capacity and the quantity of carbon accumulated were determined as a function of time under reaction conditions. Isotopic tracer techniques were used in conjunction with temperature-programmed surface reaction (TPSR) to study changes in the reactivity of CO and the different forms of carbon accumulated on the catalyst.

EXPERIMENTAL

Four titania supports were used for this study: Degussa P-25 titania, a mixture of 30% rutile and 70% anatase; two anatase supports differing in BET surface area; and rutile. These supports are referred to as TiO_2(D), TiO_2(A1), TiO_2(A2), and TiO_2(R). TiO_2(A1) is the higher surface area anatase.

TiO_2(A1) was prepared as follows. Titanium isopropoxide ($Ti(C_3H_7O)_4$, Dupont) was added dropwise to an excess of isopropyl alcohol at 274 K over a period of 4.5 h with constant mixing. The resulting slurry was allowed to settle, and then decanted and washed with distilled water. The decanting and washing was repeated 5–6 times, and the slurry was then filtered and washed several times. The final product was ground and calcined in an O_2 atmosphere. The preparation of TiO_2(A2) was similar to that of TiO_2(A1), except that the initial step was carried out at 280 K.

TiO_2(R) was prepared according to the procedure described by Kikuchi *et al.* (*17*). Titanium tetrachloride ($TiCl_4$) was added dropwise to hot distilled water at 368 K, stirred for 1 h, and then cooled to ambient temperature. After filtration, precipitated titanium hydroxide was washed with distilled water and filtered again. The washing cycle was repeated several times and finally the precipitate was dried overnight at 383 K. To remove residual chloride impurities, the support was Soxhlet extracted with water and then calcined in pure O_2 at 673 K. Extraction and calcination were repeated three times (*18*).

The phase structure of each TiO_2 support was confirmed using Raman spectroscopy, since this technique is very sensitive to the phase of TiO_2 and can detect small proportions of anatase in the presence of rutile. By this means, it was established that TiO_2(R)

TABLE 1

Catalyst Characteristics

Catalyst	Ru (wt%)	Dispersion (%)	BET (m^2/g)	H uptake ($\mu mol/g$)	CO/H	Pore diameter (Å)
$Ru/TiO_2(D)$	3.3	15.5	47.5	51.1	1.3	213
$Ru/TiO_2(A1)$	3.7	30.9	105.4	112.5	0.8	94
$Ru/TiO_2(A2)$	3.1	40.6	76.5	125.3	0.8	120
$Ru/TiO_2(R)$	6.1	30.8	46.0	186.6	2.2	167

contained no traces of anatase and that $TiO_2(A1)$ and $TiO_2(A2)$ contained no detectable traces of rutile.

Ru was introduced onto each support by incipient wetness impregnation using an aqueous solution of $RuCl_3 \cdot 3H_2O$ (Strem). The impregnated supports were dried in air at 373 K overnight, and then sieved to -30, $+60$ mesh. Reduction of the dried products were carried out at 503 K in a flow of pure H_2. The reduction temperature was intentionally kept low to keep the catalyst in its low-temperature reduced state as much as possible (*19*). To check for complete conversion of the $RuCl_3$ to metallic Ru, the chloride content of each catalyst was determined after reduction. The chloride level in $Ru/TiO_2(D)$ and $Ru/TiO_2(A1)$ was below the detection limit (0.02%). For $Ru/TiO_2(A2)$ and $Ru/TiO_2(R)$, the levels were 0.04% and 0.07%, respectively. The weight loading of Ru was determined by X-ray fluorescence.

Table 1 summarizes the physical characteristics of each catalyst. The dispersion of the Ru was determined by H_2 chemisorption at 373 K following a 2-h reduction at 473 K. Chemisorption was carried out at 373 K because hydrogen adsorption is known to approach equilibrium slowly at room temperature (*20*), and equilibrium is attained more rapidly at this temperature (*21, 22*). A static chemisorption apparatus was used. The isotherms for total and reversible adsorption were determined and the difference between the intercepts at zero pressure was used to estimate hydrogen uptake. The CO chemisorption capacity of Ru was determined by temperature-programmed surface reaction in D_2 following reduction at 498 K in pure D_2 for 2 h. Further details concerning this procedure are discussed in the Results section. The BET surface area and pore-size distribution for each catalyst was determined from N_2 isotherms at 77 K.

H_2, CO, and He were supplied from a gas flow manifold to a low dead volume quartz microreactor. UHP H_2 (Matheson Gas) or D_2 supplied by U.C.L.B.L. were further purified by passage through a Deoxo unit (Engelhard Industries) and water was removed by a molecular sieve 13X trap. UHP CO (99.999% pure, Matheson Gas) was passed through a glass bead trap at 573 K to remove iron carbonyls, an Ascarite trap to remove CO_2, and finally a molecular sieve trap. UHP He was passed through a molecular sieve trap, and 99% ^{13}CO (Isotec Inc) was used as supplied.

The products of CO hydrogenation were analyzed by gas chromatography using a Perkin–Elmer Sigma 3B gas chromatograph equipped with a FID detector. C_1–C_{14} hydrocarbons were separated on a fused silica capillary column (0.25 mm i.d. $\times$ 50 m) coated with SE-54 (1 μm thick). Temperature programming of the column was as follows: 253 K for 5 min, 20 K/min to 523 K, and then 523 K for 10 min. Since the analysis of each loop requires 28.5 min, samples of reaction products were taken as needed,

stored at 393 K, and then introduced to the chromatograph after reaction. To accomplish this, the effluent from the reactor was routed through a 10-port, two-position valve (used either to sample the products or inject the stored sample into the chromatograph) in series with a 16 sample-loop multiposition valve (used to acquire and store the samples). Both valves were contained in heated ovens maintained at 393 K to avoid condensation of products. Operation of both valves was by motor-driven actuators connected to a personal computer (IBM-PC). The microcomputer was programmed to schedule sample acquisition and analysis at desired times. The output from the FID detector was acquired by the computer via an interface and stored at a rate of two data points per second.

During a temperature-programmed surface reaction experiment, the reactor effluent was monitored by a mass spectrometer (UTI 100C). The following masses were monitored: 15 ($^{12}CH_4$), 21 ($^{13}CD4$), 28 (^{12}CO), 29 (^{13}CO), 44 ($^{12}CO_2$), and 45 ($^{13}CO_2$). Mass spectrometer control and data acquisition were carried out by the personal computer. Using this system each mass intensity could be sampled twice a second.

For each experiment, 0.2 to 0.3 g of catalyst was loaded in the reactor. The catalyst was then reduced by slowly ramping the temperature in D_2 at 10 K/min to 503 K, and then holding at this temperature for at least 2 h. The synthesis of hydrocarbons was carried out at 1 atm using ^{12}CO and D_2. All reactions were performed at the following conditions: T = 498 K; D_2/CO = 3; P_{CO} = 50 Torr; P_{D_2} = 150 Torr; P_{He} = 560 Torr; Q = 150 cc/min. CO conversions on all the catalysts were <10%. Activity was followed as a function of reaction time (t_r) by sampling at different times after the start-up of the reaction, and data were collected up to 4 h on stream. After reaction, the catalyst was reduced at 503 K overnight.

TPSR experiments were initiated by pretreating the catalyst in one of several ways, as discussed in the Results section. The reactor was flushed with He to remove gas phase reactants and the catalyst was quenched in He to room temperature in under 1 min by blowing air over the outside of the reactor. If the uptake of CO was to be determined, the catalyst was exposed to 50 Torr of ^{13}CO in He for 5 min, and then flushed in pure He. The final step in each TPSR experiment was to ramp the catalyst temperature at 0.17 K/s to 503 K in flowing D_2 (50 Torr). During this period, the evolution of ^{13}C labeled products (including ^{13}CO and $^{13}CD_4$) was monitored by the mass spectrometer.

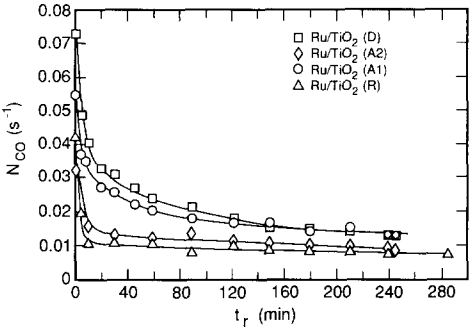

FIG. 1. CO turnover frequency as a function of reaction time. Reaction Conditions: P_{D_2} = 150 Torr, P_{CO} = 50 Torr, T = 498 K.

RESULTS

Figure 1 shows a plot of the turnover frequency for CO conversion to hydrocarbons, N_{CO}, as a function of time under reaction conditions, for each of the four catalysts. N_{CO} was determined by summing the rate of formation of C_1 through C_{14} hydrocarbons weighted by the carbon number and dividing this sum by the moles of surface Ru atoms determined by hydrogen chemisorption. Each of the catalysts exhibits a rapid initial loss in activity which is then followed by a much slower decline. The initial activity could be restored by D_2 reduction at 498 K and the plots of N_{CO} versus time could be reproduced over several cycles of reduction and reaction. It was also observed that the room-temperature uptake of CO after reduc-

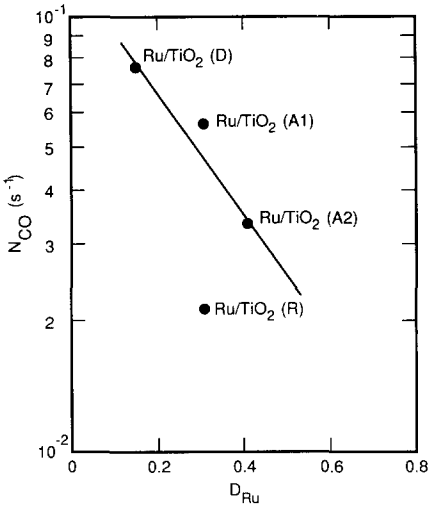

FIG. 2. Catalyst activity at 1 min after reaction start-up versus ruthenium dispersion.

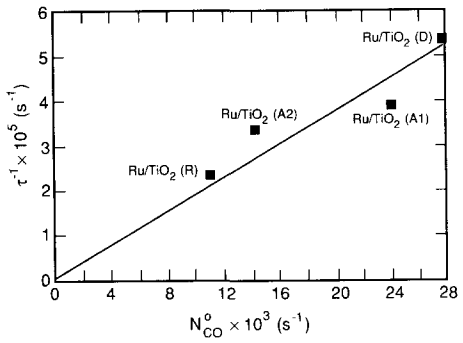

FIG. 3. Correlation of the inverse of the deactivation time constant with the CO turnover frequency at t_r = 0 obtained by extrapolation of the N_{CO} versus t_r curve for $t_r \geq 20$ min.

tion of the partially deactivated catalysts was identical to that prior to reaction.

The initial activity at t_r = 1 min for Ru/TiO_2(D), Ru/TiO_2(A1), and Ru/TiO_2(A2) exhibits an inverse linear correlation with Ru dispersion, as shown in Fig. 2. The point for Ru/TiO_2(R) lies well below the correlation. For $t_r > 20$ min, the loss in activity can be fit by an exponential function, $N_{CO} = N_{CO^0} \exp(-t_r/\tau)$, where N_{CO^0} is the apparent initial activity at $t_r = 0$ min and τ is the time constant for deactivation. The values of τ are 310 min for Ru/TiO_2(D), 420 min for Ru/TiO_2(A1), 500 min for Ru/TiO_2(A2), and 714 min for Ru/TiO_2(R). Figure 3 shows that a linear correlation exists between τ^{-1} and N_{CO^0}, which suggests that whatever causes the slow deactivation of the catalyst is produced by the catalyst itself.

Figure 4 shows an Anderson–Schulz–Flory (*23*) plot of the distribution of C_1 through C_{14} hydrocarbons for t_r = 5 min and t_r = 120 min for Ru/TiO_2(D). It is evident that the carbon number distribution of products is not strongly affected by deactivation. Similar observations were also made for the other three catalysts. Moreover, for all four catalysts, the probability of chain growth, α, was found to be 0.7 ± 0.01, indicating that α is independent of Ru dispersion and support properties (i.e., TiO_2 phase and surface area). The effects of reaction time on the proportions of total olefins, internal olefins, and branched products was examined at each carbon number between 2 and 7. For a given carbon number, the fraction of α-olefins was observed to rise during the first 10 min, at the same time that the fraction of β-olefins declined by an equivalent amount; however, neither the proportion of total olefins nor the proportion of branched products changed significantly with reaction time.

The CO adsorption capacity of each catalyst was measured both prior to the onset of reaction and after progressively longer

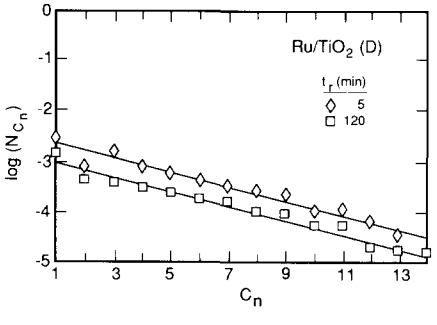

FIG. 4. Effect of reaction time on the ASF plot (log N_{C_n} vs C_n) for Ru/TiO_2(D). N_{C_n} is the turnover frequency for products of carbon number n.

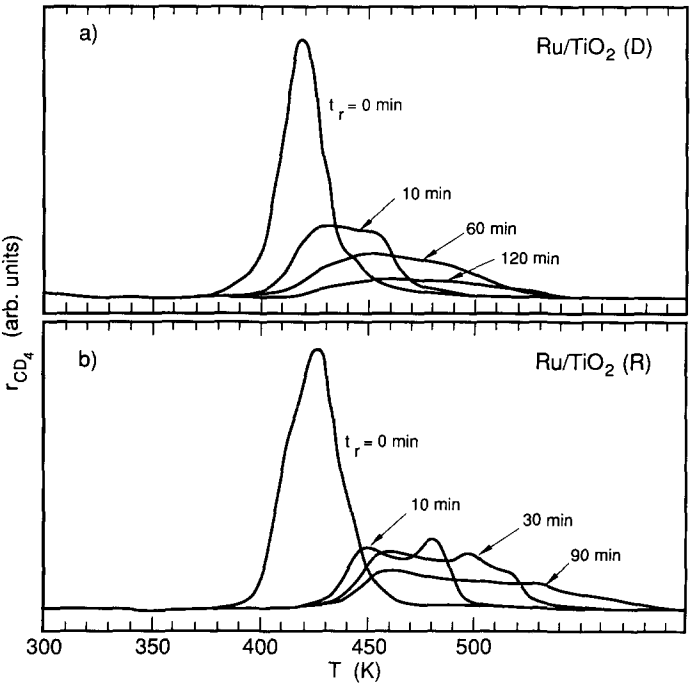

FIG. 5. ^{13}C TPSR spectra to estimate CO uptake as a function of t_r. (a) Data for Ru/TiO_2(D). (b) Data for Ru/TiO_2(R). Reaction conditions: P_{D_2} = 150 Torr, P_{CO} = 50 Torr, T = 498 K. Gas introduction sequence: $^{12}CO + D_2$ (t_r) → He (cool) → ^{13}CO (5 min) → D_2 (TPSR). In the TPSR spectra, the temperature is raised from room temperature to 503 K at 0.17 K/s and then maintained constant at 503 K.

periods of time under reaction conditions. The CO uptake of a freshly reduced catalyst was determined by exposing it to ^{13}CO at room temperature for 5 min, flushing the catalyst with He for 15 min, and then carrying out a temperature-programmed surface reaction in D_2. A peak of $^{13}CD_4$ was observed. To estimate the CO adsorption capacity after reaction, reaction was carried out in a mixture of $^{12}CO/D_2$ for a specified time after which the catalyst was cooled abruptly to room temperature in flowing He. The ^{12}CO remaining on the catalyst surface was displaced by exposing the catalyst to ^{13}CO for 5 min. The catalyst was then flushed in He for 15 min and a temperature-programmed surface reaction was carried out in flowing D_2.

The only ^{13}C-labeled product observed during the temperature-programmed surface reaction of adsorbed ^{13}CO was $^{13}CD_4$. As can be seen in Fig. 5, the amount of $^{13}CD_4$ formed decreases with increasing t_r. This change is accompanied by a progressive upscale shift in the temperature of the maximum rate of $^{13}CD_4$ formation. It is also apparent, particularly for Ru/TiO_2(R), that the $^{13}CD_4$ spectrum for $t_r > 0$ consists of two or more overlapping peaks. The apparent activation energy for the reduction of adsorbed ^{13}CO was estimated from a plot of the log of the initial rate of $^{13}CD_4$ formation versus inverse temperature. A value of 30 ± 2.5 kcal/mol was obtained for all of the catalysts, independent of t_r.

The area under the $^{13}CD_4$ peaks obtained during temperature-programmed surface reaction of ^{13}CO is taken as the measure of the CO adsorption capacity of Ru. Figure 6 shows that as t_r increases, the CO adsorp-

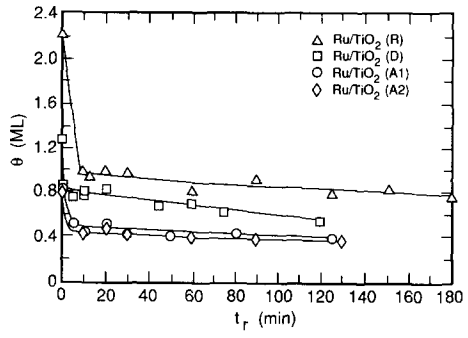

FIG. 6. CO uptake as a function of reaction time, t_r.

tion capacity of each of the four catalysts decreases rapidly and then declines more slowly for $t_r \geq 5$ min. As can be seen from Table 2, the time constants for the slow loss of CO adsorption capacity are virtually identical to those for the slow loss in CO hydrogenation activity.

Additional experiments were performed to determine the cause of the immediate loss of CO chemisorption capacity upon initiation of CO hydrogenation. The freshly reduced catalyst was exposed to ^{13}CO at room temperature for 5 min, flushed in He for 5 min, and then contacted with ^{12}CO in He for 5 min to exchange off all the adsorbed ^{13}CO. The catalyst was then flushed with He and TPSR in D_2/He was initiated. A pulse of $^{13}CO_2$ was observed when the catalyst contacted with ^{13}CO, and a peak of $^{13}CD_4$ was observed during TPSR. Both of these observations suggest that some of the adsorbed ^{13}CO disproportionates via the reaction:

TABLE 2

Comparison of the Time Constants for the Decay in N_{CO} with That for the Decay in θ_{CO}, for $t_r > 20$ Min

Catalyst	N_{CO} decay (min)	θ_{CO} decay (min)
Ru/TiO_2(D)	310	306
Ru/TiO_2(A1)	420	476
Ru/TiO_2(A2)	500	550
Ru/TiO_2(R)	714	715

TABLE 3

Comparison of the Initial Loss in θ_{CO} with That Due to Room Temperature Disproportionation of CO

Catalyst	Loss on running reaction (ML)	Room temp. disprop. CO (ML)
Ru/TiO_2(D)	0.45	0.47
Ru/TiO_2(A1)	0.33	0.27
Ru/TiO_2(A2)	0.35	0.34
Ru/TiO_2(R)	1.23	0.13

$2CO_s \rightarrow C_s + CO_2(g)$. As shown in Table 3, the amount of $^{13}C_s$ deposited by CO disproportionation correlates well with the immediate loss of CO chemisorption capacity observed upon initiation of CO hydrogenation over Ru/TiO_2(D), Ru/TiO_2(A1), and Ru/TiO_2(A2). Similar results have been reported by Yamasaki *et al.* (*7*) who observed that CO disproportionation caused a reduction in the extent of CO adsorption. For Ru/TiO_2(R), the loss in CO chemisorption capacity is much greater than the amount of carbon deposited by room-temperature disproportionation of CO. It is also observed that the amount of carbon deposited on Ru/TiO_2(R) by CO disproportionation is significantly less than that deposited on the other three catalysts.

The accumulation of carbonaceous species on the catalyst was determined using the following procedure. Reaction was run for a specified duration using a feed mixture of ^{13}CO and D_2. The catalyst was then exposed for 30 s to ^{12}CO in He, to exchange the adsorbed ^{13}CO for ^{12}CO (*13*), after which the catalyst was rapidly cooled to room temperature in flowing He. Temperature-programmed surface reaction was then carried out in flowing D_2 and the formation of $^{13}CD_4$ was monitored as a function of time. Spectrum (b) in Fig. 7 shows the rate of $^{13}CD_4$ formation versus the temperature for the case of Ru/TiO_2(D). Spectrum (a) shows the rate of $^{13}CD_4$ formation if the exchange of adsorbed ^{13}CO for ^{12}CO is eliminated from the procedure. The area under spectrum (b)

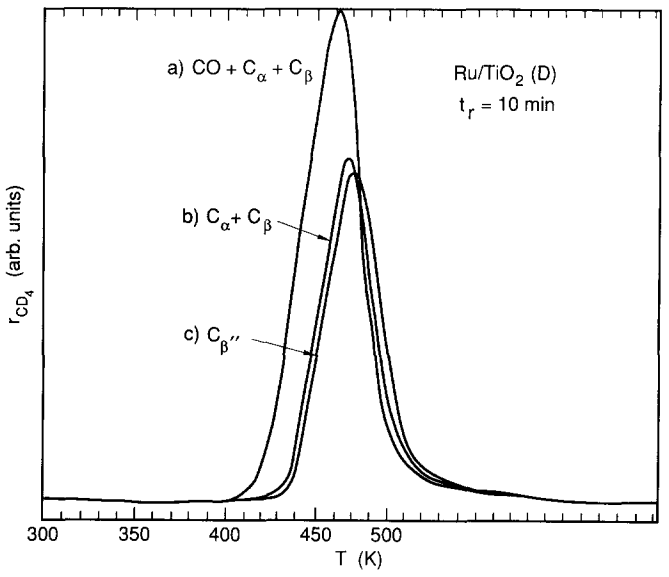

FIG. 7. ^{13}C TPSR spectra to estimate carbon accumulation on the catalyst at t_r = 10 min, standard reaction conditions. (a) CO + C_α + C_β. Gas introduction sequence: ^{13}CO + D_2 (10 min) → He (cool) → D_2 (TPSR). (b) C_α + C_β: Gas introduction sequence: ^{13}CO + D_2 (10 min) → ^{12}CO + He (30 s) → He (cool) → D_2 (TPSR). (c) C_β''. Gas introduction sequence: ^{13}CO + D_2 (10 min) → ^{12}CO + D_2 (2 min) → He (cool) → D_2 (TPSR). In the TPSR spectra, the temperature is raised from room temperature to 503 K at 0.17 K/s and then maintained constant at 503 K.

corresponds to the total amount of carbonaceous species present on the catalyst, namely, the sum of C_α and C_β, whereas the area under spectrum a also includes the amount of chemisorbed CO.

As discussed by Yokomizo *et al.* (*14*), the C_β pool of carbon can be subdivided into two pools: a C_β' pool corresponding to alkyl precursors to C_{2+} products and a C_β'' pool corresponding to alkyl groups produced by reaction, but not associated with the formation of C_{2+} products. The amount of C_β'' was determined using the following procedure. The reaction was run in a mixture of ^{13}CO and D_2 for a time t_r. The feed was then switched to a mixture of ^{12}CO and D_2 for 2 min. Experiments performed to determine the reaction time required for the latter step showed that within 2 min, the adsorbed ^{13}CO would be displaced by ^{12}CO and all the 13-labeled carbon in the C_α and C_β' pools would be replaced by ^{12}C, but that the ^{13}C carbon in the C_β'' pool would remain. After reaction in the $^{12}CO/D_2$ mixture, the catalyst was rapidly cooled to room temperature in He, and a temperature-programmed surface reaction was then carried out in flowing D_2. Spectrum (c) in Fig. 7 shows the resulting trace of $^{13}CD_4$ formation as a function of temperature. The small difference in the areas under spectra (c) and (b) represents the amount of C_α + C_β' carbon accumulated on the catalyst. Figure 8 shows that the amount of C_β'' builds up monotonically as t_r increases.

The accumulation of C_α, C_β', and C_β'' during the first 20 min of reaction are shown in Fig. 9. It is evident that the surface concentration of C_α and C_β' is less than 1 ML in most cases. For Ru/TiO_2(R), Ru/TiO_2(A1), and Ru/TiO_2(D), the accumulation of these forms of carbon passes through a maximum as t_r increases. Much larger quantities of C_β'' are formed on the catalyst surface and these species increase in quantity monotonically, and after 20 min of reaction can be as

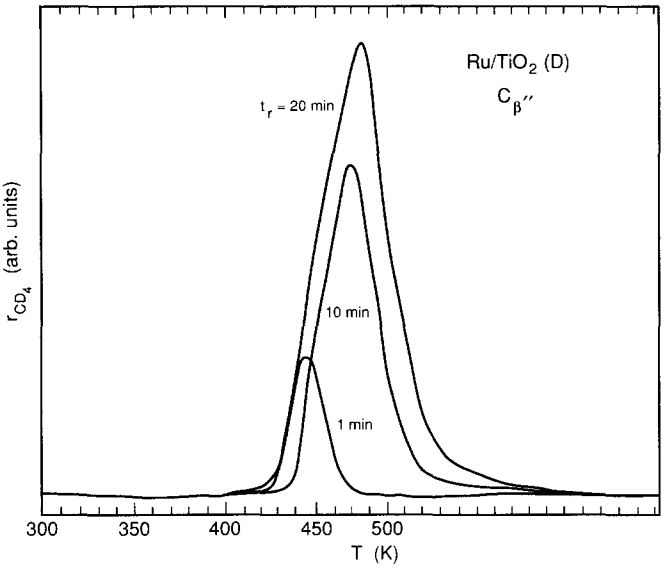

FIG. 8. ^{13}C TPSR spectra for C''_β with varying reaction time t_r. Gas introduction sequence: $^{13}CO + D_2$ (t_r) → $^{12}CO + D_2$ (2 min) → He(cool) → D_2 (TPSR). In the TPSR spectra, the temperature is raised from room temperature to 503 K at 0.17 K/s and then maintained constant at 503 K.

high as 7 ML equivalents. The time constant for the buildup of $C_\alpha + C_\beta$ during the first 10 min of reaction is listed in Table 4 and is compared with the time constant for the loss in CO hydrogenation activity during the same period. It is apparent that the time constants for the two phenomena are virtually identical, suggesting that the loss in CO hydrogenation activity during the initial stages of reaction can be attributed to the rapid buildup of C_α and C_β on the catalyst surface.

DISCUSSION

Previous investigations have shown that the specific activity of Ru for Fischer–Tropsch synthesis decreases with increasing Ru dispersion (*24, 25*). A similar trend has been observed in the present study for the CO turnover frequency measured after 1 min and for the turnover frequency determined by extrapolation of the slowly deactivating portion of the activity versus time plots (see Fig. 1). As can be seen in Fig. 2, with the exception of the point for Ru/TiO_2(R), all of the data fall along a single line, suggesting that the surface area of titania does not affect the specific activity of Ru. The deviation of the point for Ru/TiO_2(R) is believed to be due to the higher chloride content of this catalyst relative to the other three. Cl impurities can inhibit the catalytic activity of Ru for CO hydrogenation (*26*). Iyagba *et al.* (*26*) have shown that for a fixed Ru dispersion, the turnover frequency for CO hydrogenation decreases with increasing initial levels of chloride impurity. Based on their results, it is estimated that the Cl impurity in the Ru/TiO_2(R) catalyst could be expected to reduce the activity of this catalyst by about a factor of 2. This is nearly the same as the ratio of turnover frequencies for Ru/TiO_2(A1) and Ru/TiO_2(R), which have identical dispersions.

To determine whether the decrease in turnover frequency with increasing Ru dispersion is dependent on the support composition, a comparison was made between Ru/TiO_2 and Ru/Al_2O_3 catalysts. Figure 10 shows the turnover frequencies for methane obtained in the present study and similar results obtained by Kellner and Bell (*25*)

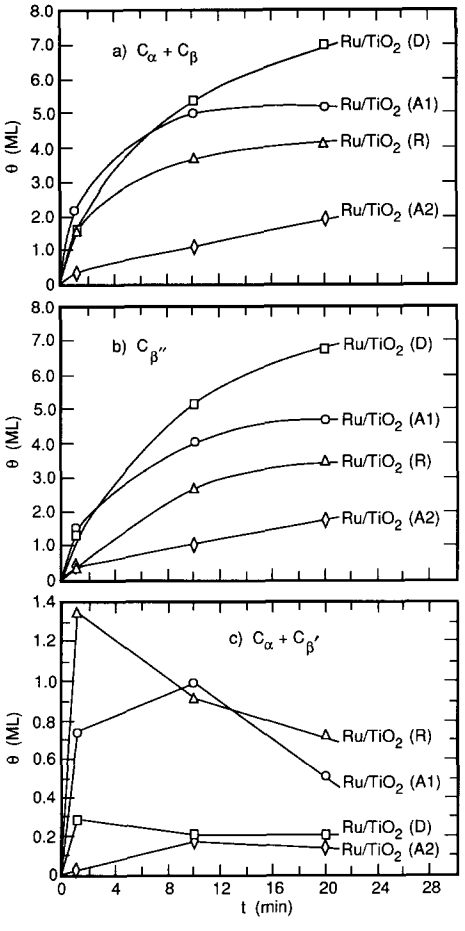

FIG. 9. Coverages of carbon species obtained from ^{13}C TPSR as a function of reaction time. (a) $C_\alpha + C_\beta$. (b) C''_β. (c) $C_\alpha + C'_\beta$.

using Ru/Al_2O_3 catalysts. It is evident that the slopes of the two sets of data are identical, indicating that the decrease in turnover frequency with increasing dispersion is an intrinsic function of the Ru particle size, independent of the support composition. Figure 10 shows as well that at a fixed Ru dispersion, the methane turnover frequency is two times higher for titania-supported Ru than for alumina-supported Ru. Since the weight ratio of C_{2+} products to methane is roughly a factor of 5 higher for the titania supported catalysts, this means that the CO turnover frequency for the titania-supported catalysts is approximately a factor of 10 higher than that for alumina-supported Ru.

The higher activity of TiO_2-supported Ru to Al_2O_3-supported Ru can be attributed to effects of highly active sites located at the boundaries of TiO_x islands partially covering the Ru metal surface (*27*). The identical dependence of the methane turnover frequency on Ru dispersion for Ru/TiO_2 and Ru/Al_2O_3, shown in Fig. 10, suggests that the TiO_x coverage of Ru is probably independent of Ru dispersion in the dispersion range studied. XPS studies (*28*) have suggested that the partial reduction of TiO_2 produces Ti^{3+} sites which can then interact with the oxygen of CO adsorbed on metal atoms immediately adjacent to the Ti^{3+} ions. This mode of CO adsorption has been proposed to weaken the C–O bond, and hence facilitate its cleavage, an important first step in CO hydrogenation (*29–35*).

Kellner and Bell (*25*) have attributed the decrease in specific activity with increasing Ru dispersion to a geometric effect. They note that an essential step in the hydrogenation of CO to hydrocarbons is the dissociation of adsorbed CO. Indirect evidence suggests that this process occurs preferentially on flat metal surfaces, rather than on low coordination sites occurring at the corners and edges of metal particles (*36, 37*). Since the proportion of surface metal sites occurring on flat planes decreases with increasing metal dispersion, it is possible to explain the results shown in Fig. 10. The

TABLE 4

Comparison of the Time Constants for the Accumulation of $C_\alpha + C_\beta$ with That for the Decay in N_{CO} during the First 10 Min under Reaction Conditions

Catalyst	$(C_\alpha + C_\beta)$ (min)	N_{CO} (min)
Ru/TiO_2(D)	6.1	6.3
Ru/TiO_2(A1)	8.3	8.7
Ru/TiO_2(A2)	6.2	7.8
Ru/TiO_2(R)	8.3	8.3

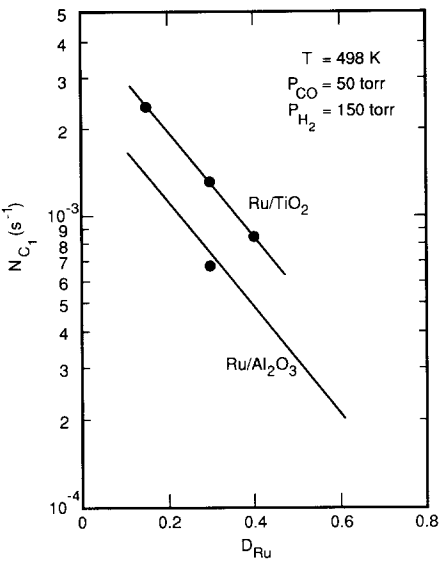

FIG. 10. Comparison of methane turnover frequency from this work over Ru/TiO_2 and Ru/Al_2O_3 (*25*). All data are based on measurements made using a H_2/CO feed mixture.

postulation of CO dissociation as a rate-determining step in CO hydrogenation is also consistent with the observed distribution of products. As noted in the preceding section, the probability of chain growth, α, is independent of Ru dispersion. This together with the absence of any effect of dispersion on the olefin to paraffin ratio or the extent of chain branching suggests that the only step in the reaction sequence affected by Ru particle size is the initial process of CO dissociation.

The importance of CO dissociation in CO hydrogenation is also borne out by the observation that the room-temperature disproportionation of CO is most extensive on the catalyst exhibiting the highest initial activity, Ru/TiO_2(D), and is least extensive on the catalyst with the lowest initial activity, Ru/TiO_2(R) (see Table 3). Furthermore, the observation of room-temperature CO disproportionation on Ru/TiO_2 indicates a higher activity for these catalysts compared to silica-supported Ni, Co, and Ru, which require temperatures of at least 423 K (*38*).

All four Ru/TiO_2 catalysts exhibit very similar deactivation behavior with time under reaction conditions. There is a very rapid loss of activity during the first 20 min or so, whereafter the activity declines much more slowly. Deactivation does not change the product carbon number distribution; the product selectivity is independent of the degree of deactivation, the dispersion of Ru, and the phase of the titania support. Comparison of the data in Figs. 1 and 6 shows that the loss in synthesis activity is accompanied by a loss in CO chemisorption capacity. Hydrogen reduction of the catalyst fully restores the initial activity of the catalysts as well as their CO chemisorption capacity. This indicates that the loss in activity is reversible and does not appear to be associated with a decrease in metal dispersion.

For very short reaction times ($t_r \leq 1$ min), the loss in Ru activity can be attributed to the accumulation of C_α. As noted earlier, this species is a precursor to the formation of hydrocarbons. However, the increase in coverage of C_α will result in a loss in CO chemisorption capacity. This is also shown in Table 3. Hoffmann and Robbins (*39*) have also observed a loss in CO chemisorption capacity during CO hydrogenation over Ru(001) due to the formation of surface carbon. Figure 9c shows, though, that the coverage of $C_\alpha + C'_\beta$ rapidly passes through a maximum with reaction time. For reaction times longer than a few minutes, the coverage by C''_β becomes significant, and it is probably this species which is primarily responsible for the loss in catalytic activity and CO chemisorption capacity at longer reaction times. The TPSR spectra presented in Fig. 8 indicate that C_β does not undergo hydrogenolysis until much of the chemisorbed CO has been removed from the surface, in agreement with earlier observations by Kobori *et al.* (*40*) and Zhou and Gulari (*16*). It has been proposed (*16, 41, 42*) that the stability of alkyl groups in the C''_β pool is due to the stabilization of CO adsorbed on the same, or nearby, sites. It is interesting to

note in this context that Akhter and White (*41*) have reported a similar stabilization of ethylidyne by adsorbed CO on a Ni(111) surface.

The loss in catalytic activity for longer reaction times is attributed to the progressive accumulation of C_α and C_β. This explanation is suggested by the similarity in the time constants for the accumulation of C_α and C_β, and the time constant for deactivation during the first 10 min of reaction (see Table 4). While the results of the present study do not provide direct evidence of a correlation between activity loss and the accumulation of carbon for reaction times in excess of 20 min, one can infer such a relationship from the observed correlation between the loss in CO chemisorption capacity and activity (see Table 2), since the loss in CO chemisorption capacity is ascribable to the accumulation of carbonaceous species.

Further support for the idea that the slow deactivation is due to species produced by the catalyst can be drawn from Fig. 3. This figure shows that the rate of deactivation for $t_r > 20$ min increases linearly with the turnover frequency of the catalyst. For Ru/TiO_2(D), Ru/TiO_2(A1), and Ru/TiO_2(A2), the differences in the turnover frequency are due to differences in Ru dispersion (see Fig. 2). As discussed above, the lower than anticipated activity of Ru/TiO_2 is attributed to the higher initial Cl impurity of this catalyst relative to the other three investigated.

Finally, one might ask whether the observed loss in activity might be due to the progressive accumulation of wax either on the surface of Ru particles or in the catalyst pores. To address this question, estimates were made of the wax accumulation after 2 h of reaction. The carbon number threshold for condensation of wax was determined using an extrapolation of the measured ASF distribution together with the Kelvin equation and known vapor pressures of alkanes. For the conditions of the present experiments, it was found that all products with 28 carbon atoms or more would condense in 10 Å pores, whereas all products with 83 carbon atoms or more would condense in 100 Å pores. The total wax accumulation could then be calculated for each catalyst using the measured pore-size distribution. By this means, it was found that the wax could occupy between 0.06 and 0.55% of the pore volume in the four catalysts studied. If the wax is assumed to cover the Ru particles in a maximal fashion, then it is estimated that between 3 and 7% of the exposed Ru sites would be covered. These figures are to be compared with fractional activity losses of 23–46% over the same period of time. This suggests that wax accumulation cannot account for a significant part of the loss in activity under the conditions used in this study. Of further note is the fact that the estimated amount of wax accumulation is only 1–4% of the amount of carbon removed from the catalyst surface after reaction.

CONCLUSIONS

Titania-supported Ru catalysts undergo deactivation during CO hydrogenation, but exhibit no change in product selectivity with time on stream. The initial activity can be restored by reduction in H_2 or D_2 and there is no evidence of metal sintering due to reaction. The rate of deactivation is most rapid during the first 20 min after the start-up of reaction and declines to a much smaller rate for reaction times longer than 20 min. The long-term rate of deactivation is proportional to the activity of the catalyst, obtained by extrapolation of the long-term activity data. The loss in activity is paralleled by a loss in CO chemisorption capacity, and for reaction times longer than 20 min, the ratio of the CO turnover frequency to the CO coverage remains constant. Differences in the initial activity of Ru supported on Degussa P-25 and anatase can be attributed to differences in Ru dispersion, with higher dispersion contributing to a decrease in CO turnover frequency. For the same dispersion, Ru supported on rutile exhibits an activity two- to threefold lower than Ru supported on anatase. The lower activity of

rutile-supported Ru is attributed to the higher level of chloride impurity on rutile versus anatase. The formation of highly active sites at the boundaries of TiO_x islands located on the metal surface is proposed to be the cause for the higher activity of TiO_2-supported Ru, compared to SiO_2- or Al_2O_3-supported Ru.

Temperature-programmed surface reaction experiments show evidence of the accumulation of carbidic, C_α, and alkyl, C_β, carbon on the catalyst surface. The catalyst inventory of $(C_\alpha + C'_\beta)$ increases, passes through a maximum, and then decreases as the catalyst loses activity. On the other hand, the inventory of C''_β increases monotonically with reaction time. The accumulation of both C_α and C_β carbon results in a reduction in the CO chemisorption capacity of the catalyst. The immediate loss in CO uptake after reaction start-up is attributed to the buildup of C_α. The rapid loss in activity in the first 10 min correlates with the buildup of C_α and C_β, whereas the slower loss in activity is ascribed to the accumulation of C''_β. The alkyl chains comprising the C_β pool of carbon do not undergo extensive hydrogenolysis under reaction conditions, very likely due to inaccessibility of the chains to hydrogen as a result of CO adsorbed on adjacent sites.

ACKNOWLEDGMENTS

This work was supported by the Director, Office of Basic Energy Sciences, Chemical Sciences Division of the US Department of Energy under contract DE-AC03-76SF0098. The authors thank Dr. C. Louis and G. H. Yokomizo for the preparation of the titania supports and the catalysts, and G. T. Went for performing the Raman spectroscopy of the titania samples. The pore-size distributions and BET areas of the catalysts were obtained with the help of Dr. Leon Petrakis and Mr. B. G. Russell of Chevron Research Corporation, Richmond, CA.

REFERENCES

1. Dalla Betta, R. A., Piken, A. G., and Shelef, M., *J. Catal.* **35,** 54 (1974).
2. Dalla Betta, R. A., Piken, A. G., and Shelef, M., *J. Catal.* **40,** 173 (1975).
3. Everson, R. C., Woodburn, E. T., and Kirk, A. R. M., *J. Catal.* **53,** 186 (1978).
4. Ekerdt, J. G., and Bell, A. T., *J. Catal.* **58,** 170 (1979).
5. Moeller, A. D., and Bartholomew, C. H., *Ind. Eng. Chem. Prod. Res. Dev.* **21,** 390 (1982).
6. Bowman, R. M., and Bartholomew, C. H., *Appl. Catal.* **7,** 179 (1983).
7. Yamasaki, H., Kobori, Y., Naito, S., Onishi, T., and Tamaru, K., *J. Chem. Soc., Faraday Trans. 1* **77,** 2913 (1981).
8. Cant, N. W., and Bell, A. T., *J. Catal.* **73,** 257 (1982).
9. Winslow, P., and Bell, A. T., *J. Catal.* **86,** 158 (1984).
10. Winslow, P., and Bell, A. T., *J. Catal.* **91,** 142 (1985).
11. Duncan, T. M., Winslow, P., and Bell, A. T., *J. Catal.* **93,** 1 (1985).
12. Duncan, T. M., Reimer, J. A., Winslow, P., and Bell, A. T., *J. Catal.* **93,** 305 (1985).
13. Winslow, P., and Bell, A. T., *J. Catal.* **94,** 385 (1985).
14. Yokomizo, G. H., and Bell, A. T., *J. Catal.* **119,** 467 (1989).
15. Zhou, X., and Gulari, E., *J. Catal.* **105,** 499 (1987).
16. Zhou, X., and Gulari, E., *Langmuir* **4,** 1132 (1988).
17. Kikuchi, E., Matsumoto, N., Takahashi, T., Machino, A., and Morita, Y., *Appl. Catal.* **10,** 251 (1984).
18. Parfitt, G. D., *Trans. Faraday Soc.* **67,** 2469 (1971).
19. Tauster, S. J., Fung, S. C., and Garten, R. L., *J. Am. Chem. Soc.* **100,** 170 (1978).
20. Dalla Betta, R. A., *J. Catal.* **34,** 57 (1974).
21. Taylor, K. C., *J. Catal.* **38,** 299 (1975).
22. Kubicka, H., *React. Kinet. Catal. Lett.* **5,** 223 (1976).
23. Anderson, R. B., *in* "The Fischer-Tropsch Synthesis." Academic Press, New York, 1984.
24. King, D. L., *J. Catal.* **61,** 77 (1980).
25. Kellner, C. S., and Bell, A. T., *J. Catal.* **75,** 251 (1982).
26. Iyagba, E. J., Hoost, T. E., Nwalor, J. U., and Goodwin, J. G., *J. Catal.* **123,** 1 (1990).
27. Haller, G. L., and Resasco, D. E., *in* "Advances in Catalysis" (D. D. Eley, H. Pines, and P. B. Weisz, Eds.), Vol. 36, p. 173. Academic Press, San Diego, 1989.
28. Levin, M. E., Salmeron, M., Bell, A. T., and Somorjai, G. A., *Surf. Sci.* **195,** 429 (1988).
29. Bracey, J. D., and Burch, R., *J. Catal.* **86,** 384 (1984).
30. Anderson, J. B. F., Bracey, J. D., Burch, R., and Flambard, A. R., *in* "Proceedings, 8th International Congress on Catalysis, Berlin, 1984," Vol V, p. 111. Dechema, Frankfurt-am-Main, 1984.
31. Sachtler, W. M. H., *in* "Proceedings, 8th International Congress on Catalysis, Berlin, 1984" Vol V, p. 151. Dechema, Frankfurt-am-Main, 1984.
32. Sachtler, W. M. H., Shriver, D. F., Hollenberg, W. B., and Long, A. F., *J. Catal.* **92,** 429 (1985).

33. Vannice, M. A., and Sudhakar, C., *J. Phys. Chem.* **88,** 2429 (1984).
34. Rieck, J. S., and Bell, A. T., *J. Catal.* **99,** 262 (1986).
35. Levin, M. E., Salmeron, M., Bell, A. T., and Somorjai, A. T., *J. Catal.* **106,** 401 (1987).
36. Boudart, M., and McDonald, M. A., *J. Phys. Chem.* **88,** 2185 (1984).
37. Rieck, J. S., and Bell, A. T., *J. Catal.* **103,** 46 (1987).
38. Rabo, J. A., Risch, A. P., and Poutsma, M. L., *J. Catal.* **53,** 295 (1978).
39. Hoffmann, F. M., and Robbins, J. L., *in* "Proceedings, 9th International Congress in Catalysis, Calgary, 1988" (M. J. Phillips and M. Ternan, Eds.), Vol. 3, p. 1144. Chem. Institute of Canada, Ottawa, 1989.
40. Kobori, Y., Yamasaki, H., Naito, S., Onishi, T., and Tamaru, K., *J. Chem. Soc., Far. Trans. 1* **78,** 1473 (1982).
41. Akhter, S., and White, J. M., *Surf. Sci.* **180,** 19 (1987).
42. Akhter, S., Henderson, M. A., Mitchell, G. E., and White, J. M., *Langmuir* **4,** 246 (1988).